Peroxisome proliferator-activated receptor γ coactivator 1-α gene transfer restores mitochondrial biomass and improves mitochondrial calcium handling in post-necrotic mdx mouse skeletal muscle

Richard Godin, Frederic Daussin, Stefan Matecki, Tong Li, Basil Petrof, Yan Burelle

Peroxisome proliferator-activated receptor γ coactivator 1-α gene transfer restores mitochondrial biomass and improves mitochondrial calcium handling in post-necrotic *mdx* mouse skeletal muscle

Richard Godin[1,2], Frederic Daussin[1,2], Stefan Matecki[3], Tong Li[4], Basil J. Petrof[4] and Yan Burelle[2]

[1] *Department of Kinesiology and* [2] *Faculty of Pharmacy, Université de Montréal, Montreal, Quebec, Canada H3C 3J7*
[3] *INSERM, U1046 – Physiologie et médecine expérimentale du cœur et des muscles, Montpellier, France*
[4] *Meakins-Christie Laboratories and Respiratory Division, McGill University Health Centre and Research Institute, Montreal, Quebec, Canada H2X 2P2*

Key points

- Mitochondria are increasingly implicated in the pathogenesis of Duchenne muscular dystrophy (DMD). However, the extent to which the multiple facets of mitochondrial function are altered remains uncertain due to the lack of detailed assessment.
- Peroxisome proliferator-activated receptor gamma coactivator 1-alpha (PGC1α) was recently shown to improve muscle pathology in dystrophic muscle. However, the mechanisms are not fully elucidated.
- This study provides novel information on mitochondrial dysfunction in DMD namely that (i) loss of mitochondrial biomass precedes overt respiratory abnormalities, (ii) mitochondrial H_2O_2 metabolism is improved at a time when no oxidative damage is detectable in the muscle, and (iii) susceptibility to permeability transition pore (PTP) opening is increased, which has only been inferred in the past, but never actually measured.
- This study also provides new mechanistic information regarding the beneficial effects of PGC1α overexpression upon dystrophic muscles, namely that PGC1α not only increases mitochondrial biomass but also reduces PTP opening, improves mitochondrial Ca^{2+} handling and reduces the activation of Ca^{2+} and mitochondria-dependent proteases in muscles of *mdx* mice. These mechanisms were not examined in previous investigations, which had largely attributed the improved histopathology after PGC1α therapy to utrophin upregulation.

Abstract Alterations of mitochondrial function have been implicated in the pathogenesis of Duchenne muscular dystrophy. In the present study, mitochondrial respiratory function, reactive oxygen species (ROS) dynamics and susceptibility to Ca^{2+}-induced permeability transition pore (PTP) opening were investigated in permeabilized skeletal muscle fibres of 6-week-old *mdx* mice, in order to characterize the magnitude and nature of mitochondrial dysfunction at an early post-necrotic stage of the disease. Short-term overexpression of the transcriptional co-activator PGC1α, achieved by *in vivo* plasmid transfection, was then performed to determine whether this intervention could prevent mitochondrial impairment and mitigate associated biochemical abnormalities. Compared with normal mice, *mdx* mice exhibited a lower mitochondrial biomass and oxidative capacity, greater ROS buffering capabilities, and an increased vulnerability to Ca^{2+}-induced opening of the mitochondrial permeability transition pore complex. PGC1α gene transfer restored mitochondrial biomass, normalized the susceptibility to PTP opening and

R. Godin and F. Daussin are co-first authors. B. J. Petrof and Y. Burelle are co-senior authors.

increased the capacity of mitochondria to buffer Ca^{2+}. This was associated with reductions in the activity levels of the Ca^{2+}-dependent protease calpain as well as caspases 3 and 9. Overall, these results suggest that overexpression of PGC1α in dystrophin-deficient muscles, after the onset of necrosis, has direct beneficial effects upon multiple aspects of mitochondrial function, which may in turn mitigate the activation of proteolytic and apoptotic signalling pathways associated with disease progression.

(Resubmitted 7 August 2012; accepted after revision 17 August 2012; first published online 20 August 2012)
Corresponding author Y. Burelle: Faculty of Pharmacy, Université de Montréal, PO Box 6128, Succursalle Centre Ville, Montreal, Quebec, Canada H3C 3J7. Email: yan.burelle@umontreal.ca

Abbreviations CCCP, carbonyl cyanide *m*-chlorophenyl hydrazone; CRC, calcium retention capacity; DMD, Duchenne muscular dystrophy; ETC, electron transport chain; PGC1α, peroxisome proliferator-activated receptor gamma coactivator 1-alpha; PTP, permeability transition pore; ROS, reactive oxygen species; TA, tibialis anterior muscle.

Introduction

Duchenne muscular dystrophy (DMD) is an inherited disease resulting from mutations in the gene located at chromosome Xp21 encoding dystrophin, which leads to absence of this subsarcolemmal cytoskeletal protein from striated muscle cells (Koenig *et al.* 1987). The disease is characterized by repetitive cycles of necrosis and regeneration, which inexorably progress to overt muscle fibre loss and fibrosis as muscle repair capacities become overwhelmed (Petrof, 2002). Although much progress has been made in our understanding of DMD (Koenig *et al.* 1987), the precise mechanisms leading to disease progression still remain unclear. The instability of the sarcolemma resulting from the lack of dystrophin is clearly a major contributor to pathogenesis (Petrof *et al.* 1993*a*); however, other factors such as increased extracellular Ca^{2+} entry leading to excessive cytosolic levels, elevated oxidative stress, and exaggerated activation of proteolytic and apoptotic signalling pathways, have also been implicated (Petrof, 2002; Ruegg *et al.* 2002; Tidball & Wehling-Henricks, 2007).

Studies in DMD patients and *mdx* mice (the most frequently employed animal model of the disease) have also shown that skeletal muscles lacking dystrophin exhibit impaired oxidative phosphorylation and reduced expression levels of numerous mitochondrial genes, leading to the suggestion that energetic deficiency is involved in disease pathogenesis (Dunn *et al.* 1993; Even *et al.* 1994; Gannoun-Zaki *et al.* 1995; Kuznetsov *et al.* 1998; Chen *et al.* 2000). Perhaps more importantly, mitochondrial dysfunction can also play a direct role in many of the above-mentioned factors suggested to cause repeated muscle injury and subsequent disease progression in DMD (Burelle *et al.* 2010). In this regard, mitochondria are known to be critically involved in the spatio-temporal regulation of intracellular Ca^{2+} (Ichas *et al.* 1997; Giacomello *et al.* 2007), the regulation of reactive oxygen species (ROS) production and scavenging (Turrens, 2003), and the triggering of cell death signalling through permeabilization of their membranes (Green & Kroemer, 2004; Zamzami *et al.* 2005; Burelle *et al.* 2010). However, the extent to which these mitochondrial functions are altered in dystrophin-deficient muscle currently remains uncertain, due in part to a lack of integrative assessments of the mitochondrial phenotype. Nevertheless, mitochondria are increasingly viewed as important contributors to muscle injury in DMD, and as potential targets for novel therapeutic interventions (Burelle *et al.* 2010). In support of this notion, recent work has shown that genetic and pharmacological inhibition of a mitochondria-dependent cell death pathway, mediated through opening of the permeability transition pore complex (PTP), significantly attenuates muscle fibre necrosis in mice lacking dystrophin (Millay *et al.* 2008; Reutenauer *et al.* 2008), δ-sarcoglycan (Millay *et al.* 2008) and collagen VI (Irwin *et al.* 2003).

PGC1α is recognized as a dominant regulator of oxidative metabolism in many tissues, where it acts as a transcriptional co-activator of nuclear receptors and other transcription factors regulating adaptive mitochondrial responses as well as other biological programs linked to the oxidative state of cells (Kelly & Scarpulla, 2004). Recently, genetic crossing of *mdx* mice with transgenic animals over-expressing PGC1α in a skeletal muscle-specific fashion, as well as long-term overexpression of PGC1α in *mdx* mice using adenoassociated virus-mediated gene transfer, were both shown to improve multiple indices of dystrophic muscle pathology (Handschin *et al.* 2007; Selsby *et al.* 2012). However, the specific impact of PGC1α overexpression upon mitochondrial function *per se* has not been investigated in dystrophin-deficient muscle. Furthermore, in previous investigations PGC1α was over-expressed at the germline level or prior to the initial onset of myofibre damage (Handschin *et al.* 2007; Selsby *et al.* 2012). Therefore, these previous studies did not allow for testing of whether this approach has beneficial effects when instituted as a potential therapy after cycles of necrosis and regeneration have already begun, which is the more clinically relevant scenario.

Accordingly, in the present study we sought to determine the impact of PGC1α overexpression upon mitochondrial functional abnormalities and their downstream consequences in *mdx* muscles during the early regenerative phase, which follows the first wave of myonecrotic lesions. To this end, we first performed a comprehensive assessment of the mitochondrial functional phenotype prevailing at this time. We then proceeded to determine whether short-term overexpression of PGC1α, using plasmid-mediated gene transfer, was sufficient to rescue mitochondrial functional abnormalities. In particular, we tested the hypothesis that PGC1α could increase mitochondrial biomass and improve the ability of mitochondria to withstand and manage excessive Ca^{2+} loads, which are a central pathological hallmark of skeletal muscle fibres lacking dystrophin.

Methods

Animal care

The 6-week-old male *mdx* and C57BL/10ScSn mice originated from a colony maintained at the McGill University Health Centre (Montreal, Canada). All procedures were approved by the animal ethics committees of McGill University and the Université de Montréal and were in accordance with the guidelines of the Canadian Council of Animal Care.

Mitochondrial functional assays in permeabilized muscle fibres

Tibialis anterior (TA) muscles were sampled following killing by cervical dislocation. Dissection and permeabilization of fibre bundles with saponin were performed as described previously (Picard *et al.* 2008*a*). Ghost fibres were prepared (Picard *et al.* 2008*a*) by incubating saponin-permeabilized bundles in a high KCl medium, which allows extraction of myosin. Permeabilized myofibres and ghost fibre bundles were then kept on ice until use. All mitochondrial parameters described below were determined at least in duplicate.

Mitochondrial respiration

Mitochondrial respiratory function was determined in an oxymeter equipped with a Clark-type electrode (Oxygraph, Hansatech Instruments) as per Picard *et al.* (2008*a*). The chamber was filled with 1 ml of solution B (in mM: 2.77 CaK_2EGTA, 7.23 K_2EGTA (100 nM free Ca^{2+}), 6.56 $MgCl_2$ (1 mM free Mg^{2+}), 20 taurine, 0.5 DTT, 50 potassium methane sulfonate (160 mM ionic strength) and 20 imidazole, pH 7.1), and after recording baseline oxygen content in the chamber, one bundle of 1–2 mg dry weight of permeabilized myofibres was placed into the chamber, which was then sealed shut. Baseline readings were taken in the presence of the complex I substrates glutamate–malate (10:5 mM, V_{GM}). The following additions where then sequentially made: the complex I blocker amytal (2 mM), ADP (2 mM, V_{ADP}), the complex II substrate succinate (25 mM, V_{succ}), the uncoupler CCCP (1 μM, V_{CCCP}), the complex III blocker antimycin-A (8 μM) and the complex IV substrates *N*,*N*′,*N*′-tetramethyl-*p*-phenylenediamine dihydrochloride (TMPD)-ascorbate (0.9:9 mM, V_{TMPD}). Respiration rates were measured at 23°C under continuous stirring. At the end of each test, fibres were carefully removed from the oxygraphic cell, blotted and dried for determination of fibre weight. Rates of O_2 consumption (J_{O_2}) were expressed in nmol O_2 min^{-1} (mg dry weight)$^{-1}$.

Enzyme activities

Activities of complex I (CI, NADH-CoQ reductase), complex II (CII, succinate dehydrogenase), complex IV (CIV, cytochrome oxidase complex) and citrate synthase (CS) were measured spectrophotometrically in a plate reader using standard coupled enzyme assays as previously described (Marcil *et al.* 2006). Activities were expressed in mU min^{-1} (mg wet muscle weight)$^{-1}$. Activities of calpain, caspase 3 and caspase 9 were determined fluorimetrically on a plate reader (excitation–emission: 400–505 nm) by measuring the cleavage of Ac-LLY-AFC (Biovision), Ac-DEVD-AFC and Ac-LEHD-AFC, respectively (Enzo Life Sciences). Activities were expressed in Δfluorescence min^{-1} (μg protein)$^{-1}$.

Mitochondrial H_2O_2 release

Net H_2O_2 release by respiring mitochondria was measured in permeabilized fibre bundles with the fluorescent probe Amplex Red (20 μM: excitation–emission: 563–587 nm) as described previously (Ascah *et al.* 2011). Following preparation of permeabilized fibres, samples destined for H_2O_2 measurements were rinsed 3 times in buffer Z (in mM: 110 K-Mes, 35 KCl, 1 EGTA, 5 K_2HPO_4, 3 $MgCl_2 6H_2O$ and 0.5 mg ml^{-1} BSA, pH 7.3 at 4°C). Fibre bundles (0.3–1.0 mg dry weight) were incubated at 37°C in a quartz microcuvette with continuous magnetic stirring in 600 μl of buffer Z (pH 7.3 at 37°C) supplemented with 1.2 U ml^{-1} horseradish peroxidase. Baseline fluorescence readings were taken in the absence of any exogenous respiratory substrates. The following additions were then made sequentially: glutamate (5 mM), succinate (5 mM), ADP (10 mM) and antimycin-A (8 μM). Rates of H_2O_2 production were calculated from a standard curve

established under the same experimental conditions. All H_2O_2 measurements were performed at least in duplicate.

Mitochondrial H_2O_2 scavenging

To compare the mitochondrial H_2O_2 scavenging capacity, permeabilized fibre bundles were placed in 500 μl of buffer Z containing 50 μM pyruvate and 20 μM malate in a thermally controlled chamber set at 37°C with continuous stirring as previously described (Ascah *et al.* 2011). An aliquot of the buffer was removed immediately after adding 40 μM of H_2O_2 and subsequently at 20, 40 and 60 s. H_2O_2 content in aliquots was determined immediately on a fluorescence plate reader in a buffer containing 10 μM of Amplex Red and 0.5 U ml^{-1} horseradish peroxidase. The rate of H_2O_2 scavenging by mitochondria was determined as the difference between fluorescence levels measured at $t = 0$ and $t = 60$ s. H_2O_2 levels were calculated from a standard curve performed under identical conditions. At the end of each test, fibres were carefully removed from the microcuvette, blotted and dried for determination of fibre weight. All measurements were performed at least in triplicate and results were expressed in nmol H_2O_2 scavenged min^{-1} (mg dry weight)$^{-1}$.

Permeability transition pore opening and calcium retention capacity

Ghost fibres (0.3–1.0 mg dry fibre weight) were incubated at 23°C in a quartz microcuvette with continuous magnetic steering in 600 μl of CRC buffer (in mM: 250 sucrose, 10 Mops, 0.005 EGTA, 10 Pi-Tris, pH 7.3) supplemented with glutamate–malate (5:2.5 mM) and 0.5 nM oligomycin. Following the addition of fibres and respiratory substrates, a single pulse of 20 nmol of Ca^{2+} was added. Time for opening of the PTP was taken as the time lapse between the addition of the Ca^{2+} pulse and the time at which Ca^{2+} release was first noted. Calcium retention capacity (CRC) was defined as the total amount of Ca^{2+} accumulated by mitochondria prior to Ca^{2+} release caused by PTP opening. CRC values were expressed per mg of dry fibre weight. Ca^{2+} concentration in the cuvette was calculated from a standard curve relating $[Ca^{2+}]$ to the fluorescence of Ca-Green 5N (excitation–emmision: 505–535 nm) (Picard *et al.* 2008*b*; Ascah *et al.* 2011).

Immunoblotting

Proteins were extracted from muscle, separated by sodium dodecyl sulfate–polyacrylamide gel electrophoresis, and transferred onto polyvinylidene difluoride membranes. Protein modification induced by the lipid peroxidation byproduct 4-hydroxy-2-nonenal protein adducts (4-HNE), an unsaturated aldehyde that can bind to lysine, cysteine and histidine residues of proteins, was evaluated by reacting the membranes with an antibody directed against 4-HNE (1:1000 dilution; Alpha Diagnostic Intl. Inc., San-Antonio, TX, USA). Protein carbonylation, another index of oxidative stress, was evaluated using the Oxyblot Protein Oxidation Kit (EMD Millipore, Billerica, MA, USA). The level of cleaved caspase 3 was measured by probing the membranes with an anti-cleaved caspase 3 antibody (1:1000; no. 9664S, Cell Signalling). Mitochondrial density was assessed by probing the membranes with an antibody directed against voltage-dependent anion channels (VDAC, 1:2000 dilution; Alexis Biochemicals, San Diego, CA, USA). The expression of lactate dehydrogenase was quantified using an anti-lactate dehydrogenase (LDH, 1:1000 dilution; Santa Cruz, Santa Cruz, CA, USA) antibody. LDH was used as a loading control because the expression of this enzyme is very high in skeletal muscle and is not affected by the disease. Equal loading of samples was confirmed by Ponceau or Coomassie Blue staining. Bands were visualized by enhanced chemiluminescence (Amersham) with film exposure times ranging from 1 to 45 min. Films were scanned and bands quantified by GelEval or FluorChem 8000 software.

Histology and immunostaining

Transverse cryosections stained by haematoxylin and eosin were used for determining the percentage of centrally nucleated fibres (Briguet *et al.* 2004), with a minimum of five cross-sections per muscle each containing an average of 100 fibres. To quantify transfection efficiency, 7 μm cryosections from muscles transfected with pBud-PGC1α-Tomato and pBud-Tomato were incubated with an antibody directed against PGC1α (1:50; no. AB3242, Millipore) and a FITC-conjugated secondary antibody (1:1000; no. AF488, AlexaFluor). The slides were examined under fluorescence microscopy using fluorescein isothiocyanate filter settings, and the images were captured to computer with a cooled-CCD camera, using identical exposure parameters for all experimental conditions. Images taken at low magnification (4× Plan fluor objective) were used to quantify transfection efficiency, which was defined as the percentage of muscle area displaying increased PGC1α immunoreactivity. Quantification of PGC1α expression in transfected *vs.* untransfected fibres was quantified at higher magnification (10× Plan fluor objective).

PGC1α gene transfer *in vivo*

The murine PGC1α cDNA was cloned into the mammalian expression vector pBudCE4.1 (Invitrogen),

under the control of the human cytomegalovirus promoter; the human elongation factor 1α subunit promoter was used to separately drive constitutive expression of a tdTomato red fluorescent protein (Clontech) within the same vector (designated pBud-PGC1α-Tomato). The same plasmid, but in which the PGC1α cDNA was omitted (designated pBud-Tomato), was used as a control. Mice were lightly anaesthetized and one TA muscle was injected with a volume of 50 μl of the pBud-PGC1α-Tomato plasmid (at a DNA concentration of 1.5 μg per μl) at three equidistant sites along the muscle length. An equal volume and concentration of the control pBud-Tomato plasmid was injected into the contralateral TA in the same fashion. The injected muscles were then exposed transcutaneously with 7 mm paddle circular electrodes to electrical stimulation (175 V cm^{-1}, 8 pulses of 20 ms at 1 s intervals) using a commercial electroporator system (ECM 830; Genetronix, Inc., from BTX) (Molnar *et al.* 2004). All animals were used for experiments 7 days after transfection. In some experiments, the whole TA muscle was homogenized for the assessment of enzymatic activities or immunoblotting as described above. For other experiments requiring the use of permeabilized fibres, transfected myofibres from both pBud-PGC1α-Tomato and control pBud-Tomato muscle groups were identified by their bright red fluorescence signal under a fluorescence microscope. Muscle regions enriched with transfected fibres were then carefully dissected (Fig. 5) and permeabilized as described above.

Statistical analyses

Results are expressed as means ± SEM. Statistical differences were analysed using one-way ANOVA (Statistica package). Tukey *post hoc* tests were used to identify the significant differences between individual groups ($P < 0.05$).

Results

Muscle histology in normal and *mdx* mice

In *mdx* mice, a major wave of muscle fibre necrosis typically occurs between 3–4 weeks of age and is rapidly followed by a regenerative response that results in replacement of a large proportion of the damaged fibres by 5–6 weeks of age (Gillis, 1999). Consistent with this, TA muscle cross-sections from 6-week-old *mdx* mice presented some persistent myofibre necrosis but only in discrete foci. The major feature noted was central nucleation of muscle fibres, a hallmark of regeneration, which was evident throughout the muscle (Fig. 1*A*–*C*). However, there were no major signs of muscle fibre atrophy at this age, as reported previously (Mouisel *et al.* 2010; Kornegay *et al.* 2012).

Mitochondrial content and respiratory function in normal and *mdx* mice

To characterize the mitochondrial phenotype, enzymatic activity measurements and respirometry analyses were performed in whole muscle and permeabilized fibres. The activities of citrate synthase, and several electron transport chain (ETC) complexes (I, II and IV) as well as the expression of the outer membrane protein VDAC were all 20–35% lower in TA muscle from *mdx* mice as compared with non-dystrophic controls (Fig. 1*D* and *E*), which is indicative of a lower mitochondrial biomass. Respiration rates per unit of muscle weight were slightly but significantly lower in permeabilized TA fibres from *mdx* mice (main group effect $P < 0.05$) (Fig. 1*F*). However, this difference was absent when respiration was expressed per unit of mitochondrial marker enzyme to take into account the lower mitochondrial biomass (data not shown). As for the acceptor control ratio, and the complex II/complex I ratio, which respectively reflect the intrinsic coupling efficiency between oxidation and phosphorylation, and the relative flux capacity between complexes I and II, no differences were observed between the two mouse strains (Fig. 1*G*). Overall, these results indicate that mitochondrial biomass is reduced in early post-necrotic *mdx* muscles, but do not suggest intrinsic ETC defects within mitochondria.

Mitochondrial ROS metabolism and susceptibility to PTP opening

Since substantial alterations in the integrity of the ETC complexes are required to alter cellular respiration, overt respiratory defects are often manifested only at advanced disease stages (Burelle *et al.* 2010). For this reason, we next examined mitochondrial ROS metabolism and susceptibility to opening of the PTP, which are more rapidly altered in response to pathological conditions in muscle (Csukly *et al.* 2006; Marcil *et al.* 2006; Burelle *et al.* 2010). Figure 2*A* presents results from experiments in which mitochondrial H_2O_2 release was measured in permeabilized fibres under standardized respiratory states that allow identification of potential mechanisms of altered ROS release by the ETC. Mitochondrial H_2O_2 release was very low in the presence of the complex I substrate glutamate, which is consistent with previous reports (Anderson & Neufer, 2006; Picard *et al.* 2008*a*; Ascah *et al.* 2011). No significant difference was observed between the two mouse strains. However, under conditions which promote high rates of superoxide production by the respiratory chain (i.e. after adding

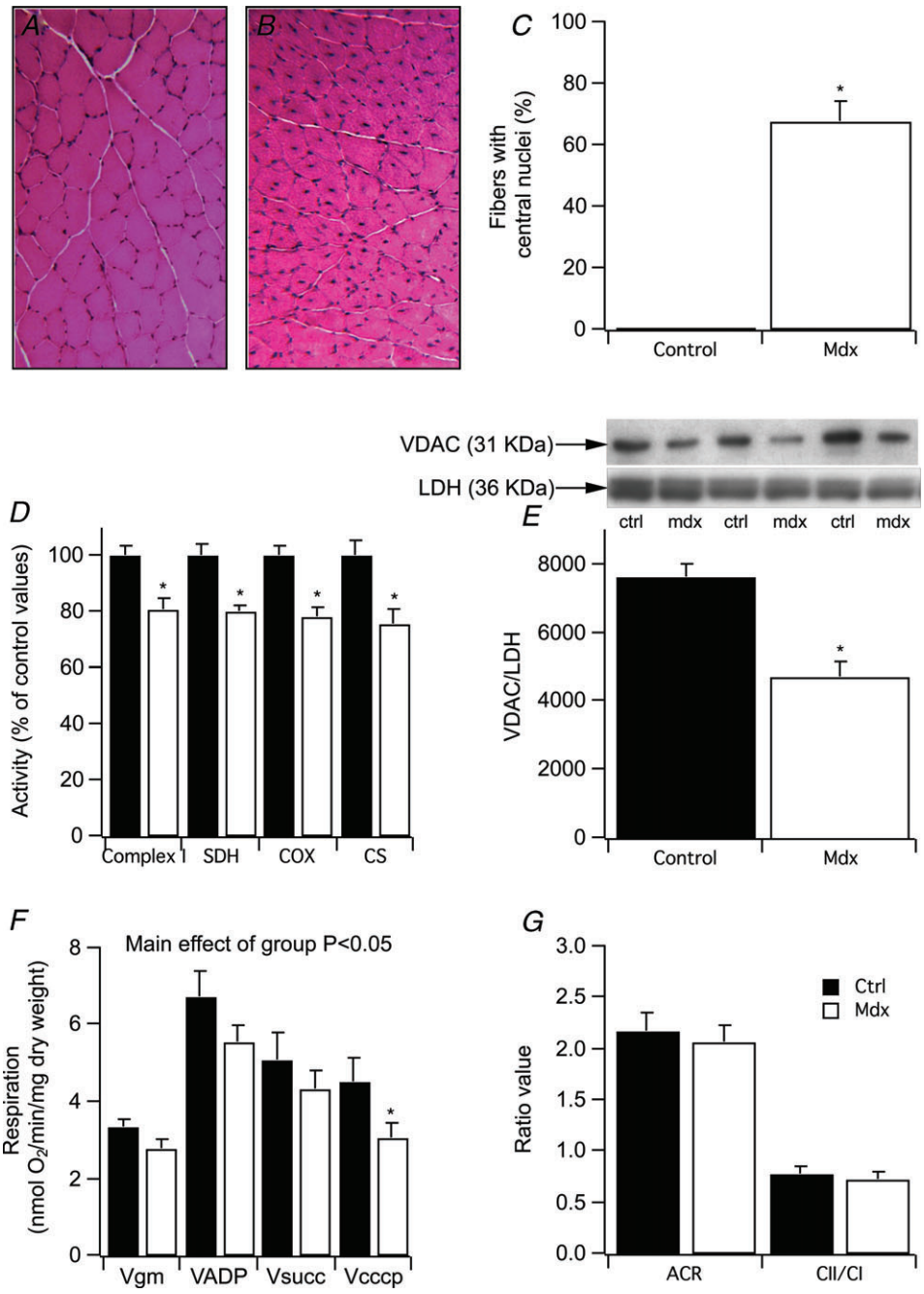

Figure 1. Muscle histology, mitochondrial density and respiratory function in normal and dystrophin-deficient muscle

A and *B*, representative cross-sections of TA muscle in 6-week-old control and *mdx* mice, respectively. *C*, proportion of muscle fibres displaying central nucleation, a hallmark of post-necrotic muscle regeneration. The analysis was performed on a minimum of 5 cross-sections per muscle each containing an average of 100 fibres. *D*, activity levels of complex I, complex II (SDH), complex IV (COX) and citrate synthase (CS) in homogenates from TA muscles. Activities were measured in mU min^{-1} (mg wet muscle weight)$^{-1}$, and expressed as a percentage of values observed in the TA of normal mice. *E*, expression of the voltage-dependent anion channel (VDAC) in whole muscle lysate normalized against the loading control LDH. *F*, respiration rates measured in permeabilized TA fibres. Following addition of fibres, the following addition sequence was performed: glutamate–malate (V_{gm}, 5:2.5 mM), ADP (V_{ADP}, 1 mM), rotenone (1 μM, not shown), succinate (V_{succ}, 5 mM) and carbonyl cyanide m-chlorophenylhydrazone (V_{CCCP}, 1 μM). *G*, acceptor control (ACR: V_{ADP}/V_{GM}) and CII/CI (V_{succ}/V_{ADP}) ratios, reflecting the coupling of oxidation to phosphorylation and the relative flux capacity between complexes I and II, respectively. Filled bars represent control values and open bars the *mdx* values ($n = 9$ in each experimental group). *$P < 0.05$, significantly different from control.

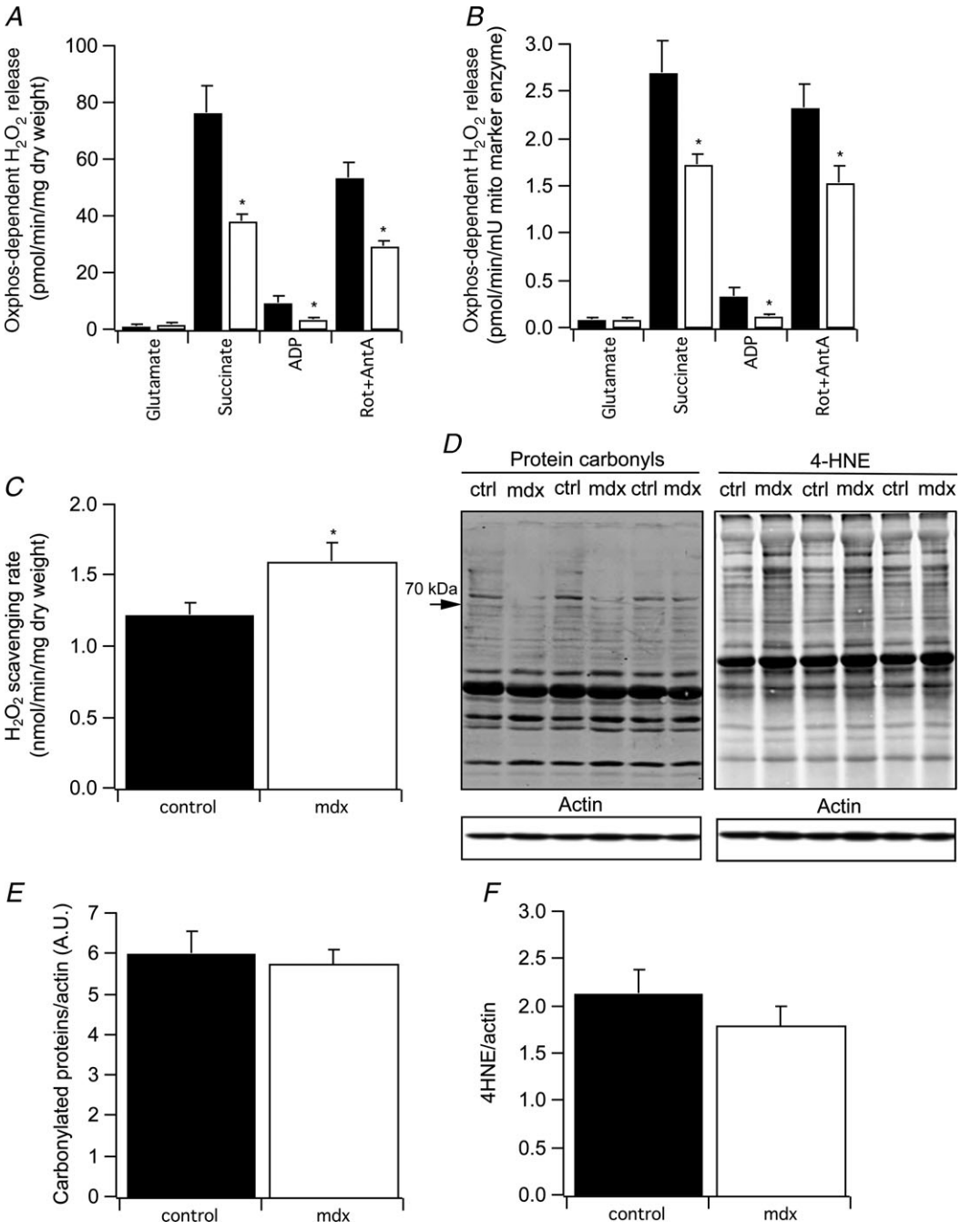

Figure 2. Mitochondrial reactive oxygen species dynamics and oxidative damage markers in normal and dystrophin-deficient muscle

A and *B*, net rate of H_2O_2 release by mitochondrial oxidative phosphorylation measured in permeabilized TA fibres. Rates of H_2O_2 release are expressed per mg of dry fibre weight (*A*) or per unit of mitochondrial marker enzyme (*B*) to take into account differences in mitochondrial biomass between groups. The protocol was as follows: after addition of the fibres, the following injection sequence was performed: glutamate (5 mM), succinate (5 mM), ADP (1 mM), rotenone + antimycin A (Rot+Ant-A: 1:8 μM). All rates presented are corrected for baseline oxidation of the Amplex red probe by fibres which was measured immediately prior to these additions. *C*, rate of H_2O_2 scavenging by succinate-energized mitochondria following addition of 20 nmol H_2O_2. All measurements were performed in parallel using 1 control and 1 *mdx* muscle per experiment ($n = 9$ in each experimental group). *D*, representative blots showing the levels of carbonylated proteins and 4-HNE adducts in whole TA muscle lysates from control and *mdx* mice at 6 weeks of age. *E*, densitometric analysis of carbonylated protein levels normalized against the loading control actin ($n = 6$ animals per group). *F*, densitometric analysis of the the 4-HNE blot normalized against the loading control actin ($n = 6$ per group). $^*P < 0.05$, significantly different from control.

the complex II substrate succinate, or after blocking complex III with antimycin-A) as well as during active phosphorylation following addition of ADP, net H_2O_2 release was significantly lower in fibres from *mdx* mice compared with their normal counterparts. Importantly, these differences were observed even after normalizing for differences in mitochondrial biomass (Fig. 2*B*), strongly suggesting adaptive changes within *mdx* mitochondria to limit oxidative stress.

To further evaluate this possibility, the rate of scavenging of an exogenous H_2O_2 load by respiring mitochondria was measured in permeabilized fibres. As shown in Fig. 2*C*, H_2O_2 scavenging fluxes were significantly higher in permeabilized fibres from *mdx* mice as compared with those of control mice, indicating a significant upregulation in the maximal capacity of the mitochondrial anti-oxidant defence system in *mdx* mice. Interestingly, as reported previously by our group (Dudley *et al.* 2006*a*,*b*), the amounts of carbonylated proteins and 4-HNE adducts were similar in the TA muscle across the two mice strains under basal conditions (Fig. 2*D*–*F*). Taken together, these findings suggest that despite any increased exposure of dystrophin-deficient muscle to ROS as previously described (Tidball & Wehling-Henricks, 2007), this remains well compensated by an adaptive anti-oxidant response at this stage of the disease.

Considering the importance of Ca^{2+} dysregulation in the pathogenesis of muscle injury in DMD (Petrof, 2002; Ruegg *et al.* 2002),the susceptibility of mitochondria to opening of the PTP and their ability to take up Ca^{2+} was next determined in permeabilized fibres using a standardized Ca^{2+} challenge. This type of assay is known to correlate well with the propensity of mitochondria to undergo permeability transition *in vivo* when challenged by stress (Javadov *et al.* 2003; Marcil *et al.* 2006). As shown in Fig. 3*A*, opening of the PTP occurred prematurely in TA fibres from *mdx* mice in comparison with fibres from control mice, indicating that mitochondria are predisposed to Ca^{2+}-induced permeability transition. The total amount of Ca^{2+} taken up by mitochondria prior to PTP opening also tended ($P = 0.07$) to be lower, mainly as

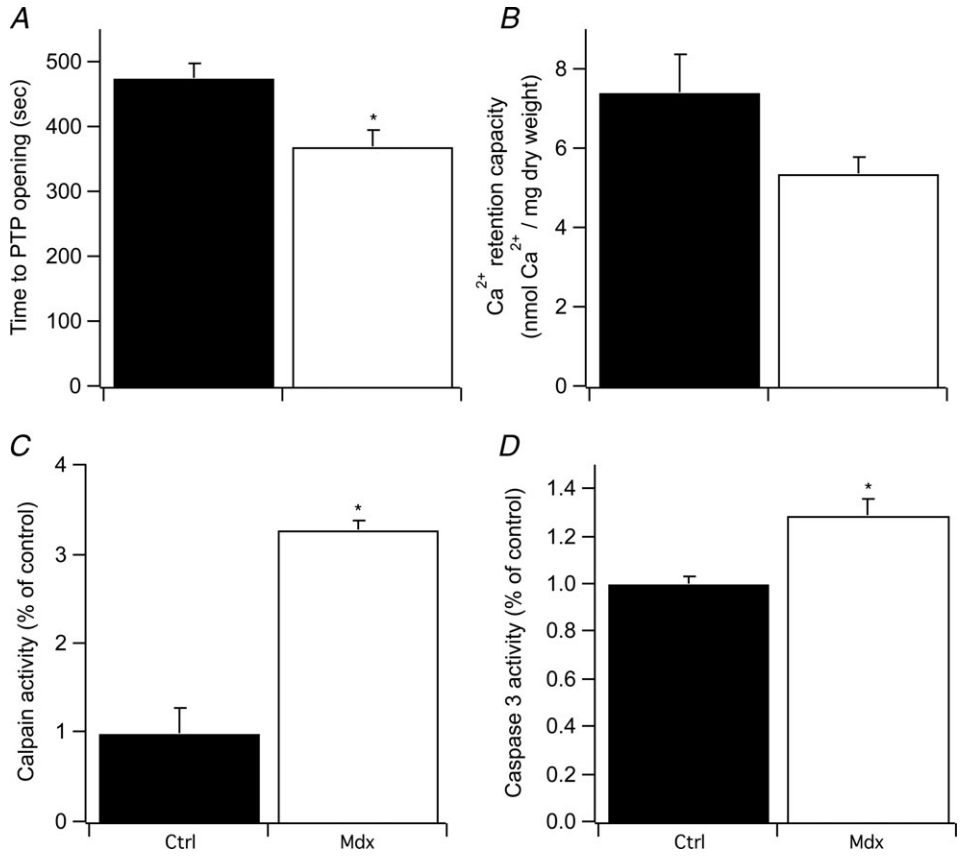

Figure 3. Susceptibility to Ca^{2+}-induced PTP opening and protease activities in dystrophin-deficient muscle

A, time required for PTP opening after the addition of a single pulse of 20 nmol Ca^{2+} to permeabilized fibres *in vitro*. *B*, total amount of Ca^{2+} accumulated by mitochondria prior to opening of the PTP ($n = 9$ per group). *C* and *D*, calpain and caspase 3 activities in whole muscle lysates ($n = 6$ per group) reported relative to values obtained in control muscles. $^*P < 0.05$, significantly different from control.

a result of the lower mitochondrial density (Fig. 3*B*). At the level of whole muscle, these observations were associated with increased activities of calpain and caspase 3 (Fig. 3*C* and *D*), which is consistent with an increased activation of Ca^{2+} and mitochondrial-dependent proteolytic signalling in dystrophin-deficient muscle.

Effect of forced expression of PGC1α on mitochondrial properties and muscle biochemistry

Following the above comprehensive characterization of mitochondrial function in *mdx* muscle, we next determined whether short-term (i.e. 7 days) over-expression of PGC1α during the post-necrotic phase could correct the main mitochondrial abnormalities observed with respect to mitochondrial biomass, PTP sensitivity and Ca^{2+} handling capabilities. The effect of PGC1α transfection on mitochondrial anti-oxidant defences was not characterized, since in TA from *mdx* mice these anti-oxidant mechanisms were already upregulated and oxidative damage was thus not apparent.

An expression plasmid (pBud-PGC1α-Tomato) encoding the murine PGC1α gene together with a separately transcribed red fluorescence Tomato marker gene was electroporated into one TA muscle, whereas the contralateral TA was transfected in the same manner with a control plasmid (pBud-Tomato) containing the marker gene alone. This electroporation procedure resulted in a 3-fold increase in PGC1α immuno-reactivity in $\sim$30% of muscles fibres at 7 days after electroporation (Fig. 4). As shown in Fig. 5, VDAC expression and the activities of all mitochondrial enzymes measured were increased by 20–35% in whole extracts from PGC1α-transfected muscles compared with those transfected with the control plasmid (Fig. 5*A* and *B*). Therefore, short-term over-expression of PGC1α was able to restore mitochondrial biomass to the level observed in normal TA muscles of non-dystrophic mice.

In addition, dissection of transfected fibres, which were identified by the Tomato marker gene expression in both control plasmid and PGC1α gene-transfected muscles (Fig. 5*C*), allowed assessment of mitochondrial susceptibility to PTP opening. Compared with the values observed in *mdx* TA fibres transfected with control plasmid, fibres transfected with the PGC1α gene exhibited a greater resistance to PTP opening when faced with an exogenous Ca^{2+} challenge. Hence, the time required to trigger PTP opening in response to Ca^{2+} increased (by 21%; Fig. 5*D* and *E*), which is comparable with the level observed in muscle fibres from healthy control mice. Furthermore, PGC1α gene transfer significantly increased (by 62%) the amount of Ca^{2+} taken up by mitochondria prior to PTP opening (Fig. 5*F*). At the level of the whole muscle, PGC1α gene transfer also reduced the activity levels of calpain, caspase 3 and caspase 9 (Fig. 5*G*). Furthermore, measurements made specifically in the regions transfected with PGC1α revealed that the levels of cleaved caspase 3 were reduced 5-fold compared with muscle regions transfected with the control plasmid (Fig. 5*H*). Therefore, these data point not only to an improvement in mitochondrial biomass following PGC1α transfection, but also to a mitigation of downstream cellular events associated with Ca^{2+} over-load and mitochondrial permeability transition, which are in turn linked to DMD pathogenesis and disease progression.

Discussion

Mitochondria are increasingly suggested to play a role in skeletal muscle pathology in DMD, and to constitute a promising target for therapy (Burelle *et al.* 2010), yet comprehensive assessments of the mitochondrial functional phenotype at defined periods of this progressive degenerative disease are lacking. Furthermore, although overexpression of PGC1α was recently shown to ameliorate muscle pathology in *mdx* mice (Handschin *et al.* 2007; Selsby *et al.* 2012), the impact of PGC1α treatment on the mitochondrial phenotype has not been addressed. In addition, PGC1α was overexpressed at the germline level or immediately after birth in prior studies, which did not permit determination of whether this approach has salutary effects when initiated after the onset of muscle necrosis. In the present study, *mdx* mice were studied during the well-defined regenerative phase that follows the initial myonecrotic wave, which allowed us to define early alterations in the mitochondrial phenotype, as well as to test whether short-term PGC1α overexpression can confer beneficial effects upon mitochondrial function in this context.

Our results reveal that muscle fibres from *mdx* mice display a complex array of mitochondrial abnormalities, including reduced mitochondrial biomass and an increased susceptibility to opening of the PTP in response to Ca^{2+} loading *in vitro*. On the other hand, an adaptive enhancement of H_2O_2 handling capabilities was also present, and intrinsic respiratory properties of the ETC did not appear to be compromised at this stage of disease. Most importantly from a therapeutic standpoint, we found that short-term overexpression of PGC1α during the early post-necrotic phase can: (1) restore mitochondrial biomass to the level observed in healthy muscle; (2) normalize the susceptibility to PTP opening; (3) enhance the mitochondrial capacity to buffer Ca^{2+}; and (4) improve downstream Ca^{2+}-related abnormalities such as excessive activation of proteolytic and apoptotic signalling pathways.

Alteration of the mitochondrial functional phenotype in dystrophin-deficient muscle

Previous studies have reported alterations in muscle energy metabolism in *mdx* mice, particularly with respect to oxidative capacity (Gannoun-Zaki *et al.* 1995; Kuznetsov *et al.* 1998; Chen *et al.* 2000). Various mechanisms have been proposed to be responsible, but there is no definite consensus. In the present study, we observed a loss of mitochondrial biomass in muscle from *mdx* mice, as indicated by the reduction in the activity/expression of several mitochondrial marker enzymes, and a mild depression of respiration rates per unit of muscle mass. However, there were no apparent signs of specific respiratory impairment, as judged by the absence of differences in respiration rates per unit of mitochondrial marker enzyme, acceptor control (V_{ADP}/V_0) ratio, and complex II/complex I ratio. These results thus suggest that early in the disease course, a loss of mitochondrial density is the main factor contributing to impaired oxidative capacity in dystrophin-deficient muscle. This loss of mitochondrial content is unlikely

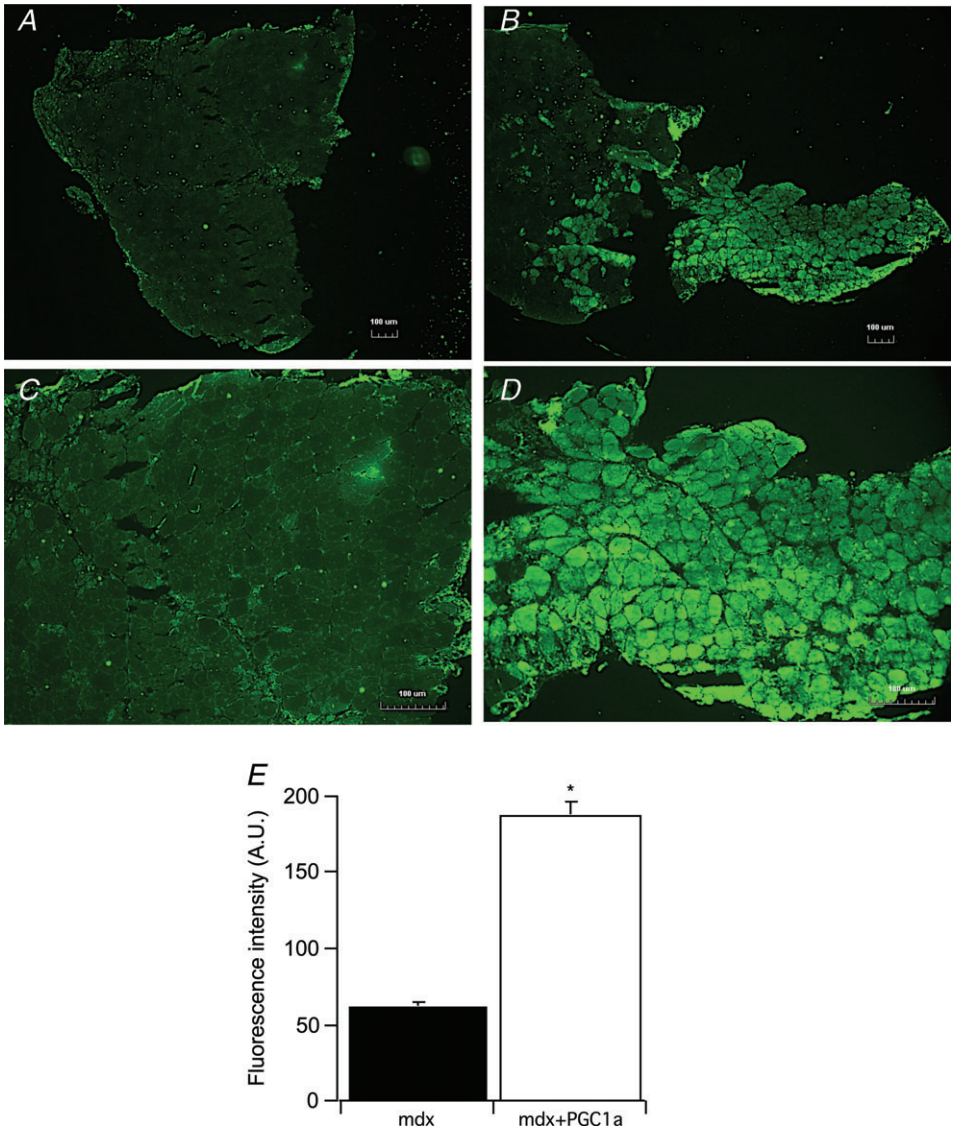

Figure 4. PGC1-α expression levels in TA muscle from dystrophin-deficient muscle transfected with PGC1α and control plasmids
A–D, PGC1-α immunoreactivity in cross-sections from *mdx* mice electroporated with the control plasmid pBud-Tomato (*A* and *C*) and the PGC1α-containing pBud-PGC1α-Tomato plasmid (*B–D*). Images were taken using a 4× (*A* and *B*) and a 10× (*C* and *D*) objective. *E*, PGC1-α immunoreactivity levels in single fibres from muscles transfected with the control plasmid (*mdx*: filled bars) *vs.* the PGC1α-containing plasmid (*mdx*+PGC1α: open bars). Data represent means ± SEM of at least 50 individual fibres in 6 different muscles injected with control or PGC1-α plasmids.

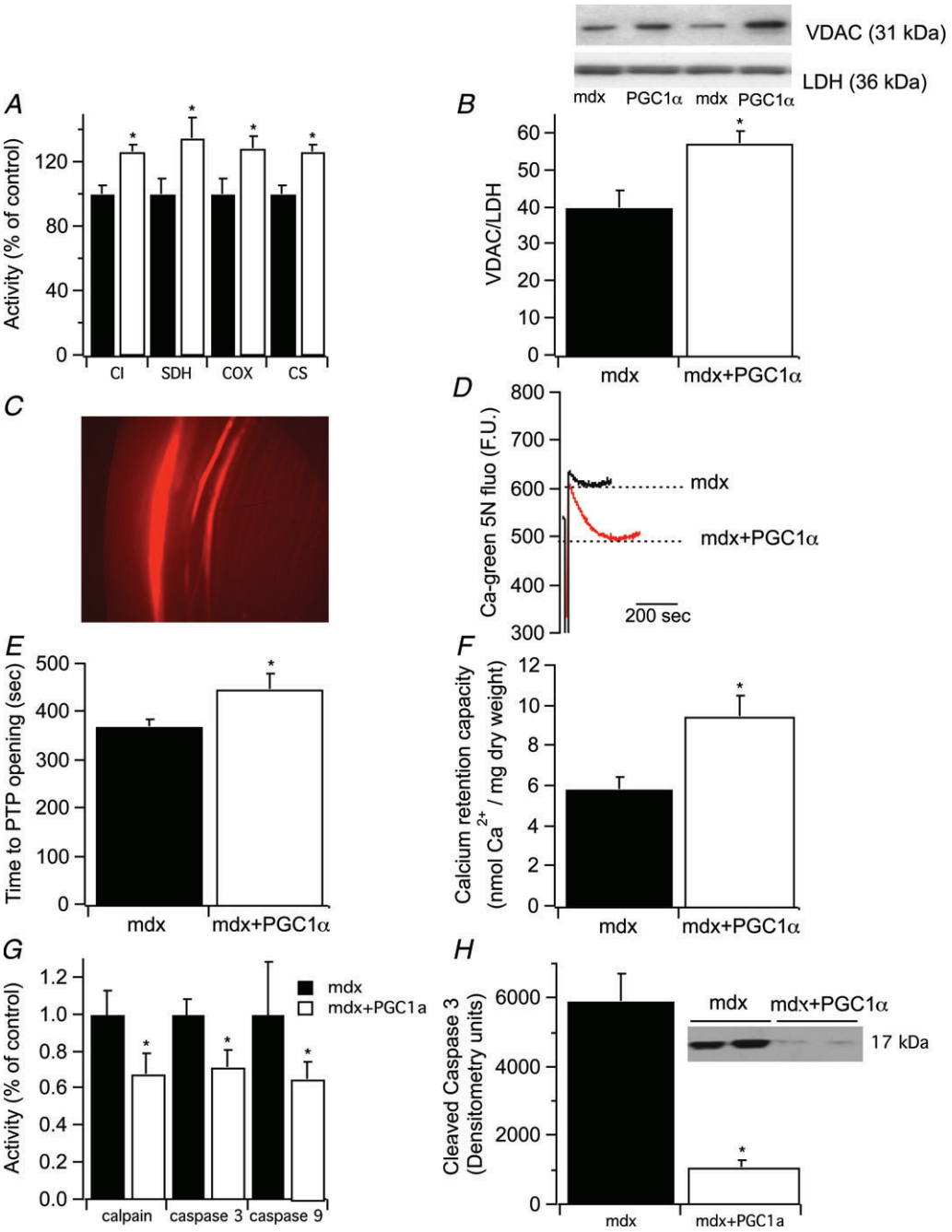

Figure 5. Effect of PGC1α gene transfer on mitochondrial oxidative capacity, Ca^{2+} handling and protease activities in dystrophin-deficient muscle

A and *B*, activities of mitochondrial marker enzymes and expression of VDAC in whole lysate from TA muscle transfected with the control plasmid pBud-Tomato (*mdx:* filled bars) *vs.* the PGC1α-containing pBud-PGC1α-Tomato plasmid (*mdx*+PGC1α: open bars) ($n = 6$ per group). *C*, representative fluorescence image at 4× magnification of a portion of the TA muscle transfected with pBud-PGC1α-Tomato. Groups of muscle fibres transfected with the plasmid are labelled in red. The muscle border is visible on the left. *D*, representative traces of Ca^{2+} uptake and release measured in ghost fibres from control and PGC1α-transfected muscle. *E*, time required for PTP opening after the addition of a single pulse of 20 nmol Ca^{2+} to permeabilized fibres *in vitro*. *F*, total amount of Ca^{2+} accumulated by mitochondria prior to opening of the PTP ($n = 6$ per group). FU; fluorescence units. *G* and *H*, activities of calpain, caspase 3 and caspase 9 (*G*), as well as levels of cleaved caspase 3 (*H*) in whole lysates from TA muscle transfected with the control plasmid pBud-Tomato *vs.* the PGC1α-containing pBud-PGC1α-Tomato plasmid ($n = 6$ per group). For each animal, the activities measured in the PGC1-α gene-transfected TA are expressed relative to the activities measured in the contralateral TA of the same animals transfected with the control pBud-Tomato plasmid. *$P < 0.05$, significantly different from control.

to be due to a lower abundance of oxidative fibres in *mdx* compared with control mice since lack of dystrophin generally leads to progressive increase in oxidative fibre content over time because of a preferential loss of fast IIbx fibres (Webster *et al.* 1988; Petrof *et al.* 1993*b*; Gillis, 1999). Presumably, at least part of this reduction of mitochondrial content at 6 weeks of age is attributable to Ca^{2+} overload and the attendant opening of the PTP. This is suggested to occur in some proportion of mitochondria (Millay *et al.* 2008; Fraysse *et al.* 2010), particularly during the peak necrotic period (i.e. between 3 and 4 weeks old), resulting in their physical disruption and rapid elimination through autophagy and the ubiquitin proteasome system (Gottlieb & Carreira, 2010; Gottlieb & Mentzer, 2011). Interestingly, several studies have reported that opening of the PTP in individual mitochondria and the resulting loss of mitochondrial membrane potential constitutes the main trigger for autophagic degradation of mitochondria (mitophagy) (Elmore *et al.* 2001; Carreira *et al.* 2010). However, more detailed studies will be necessary to test this hypothesis in dystrophic skeletal muscles.

Other studies performed on older animals (i.e. 12–24 weeks), during the more fibrotic period of the disease, have reported signs of specific respiratory abnormalities including loss of respiratory chain complexes without accompanying changes in the activity of citrate synthase (Kuznetsov *et al.* 1998), a lower acceptor control ratio (ACR) ratio (Glesby *et al.* 1988) and reduced mRNA levels for respiratory chain complex subunits without altered mitochondrial DNA content (Gannoun-Zaki *et al.* 1995). It is therefore possible that in addition to the loss of mitochondrial biomass found early in the disease, alterations in respiratory chain complex assembly or activity appear as the disease progresses, possibly as a result of repetitive bouts of increased exposure to ROS (Dudley *et al.* 2006*b*). In fact, evidence that the muscle redox status is perturbed, such as an increased glutathione disulphide/glutathione (GSSG/GSH) ratio, has been reported in 4- to 8-week-old *mdx* muscle (Dudley *et al.* 2006*a*,*b*; Tidball & Wehling-Henricks, 2007), suggesting the presence of pro-oxidant conditions during the early disease stages. However, in accordance with previously published results (Dudley *et al.* 2006*b*), we found that the levels of protein carbonyls and 4-HNE adducts were similar in muscles of control and *mdx* mice under basal conditions, indicating that if increased ROS production occurs, it is relatively well-contained and does not yet result in detectable oxidative damage.

In this regard, our results showing that mitochondria within *mdx* fibres released less H_2O_2 under standard respiratory states, and also displayed an improved capacity to eliminate H_2O_2, clearly suggest that an adaptive increase in mitochondrial ROS handling capabilities prevents overt oxidative damage within young *mdx* muscles. However, as the disease progresses, this mechanism probably becomes overwhelmed, thus allowing oxidative damage to become evident in dystrophic muscle fibres of older animals. The cellular factors responsible for stimulating this adaptive increase in mitochondrial ROS handling capacities are currently unknown. However, Ca^{2+} is capable of promoting mitochondrial ROS production by increasing the reduction state of the ETC (Brookes *et al.* 2004), as well as by triggering transient opening of the PTP (Wang *et al.* 2008). Therefore, we speculate that dysregulation of Ca^{2+}, which is a hallmark of DMD, may induce short-term localized bursts of superoxide that are insufficient to cause oxidative damage initially, but are nonetheless important enough to trigger an adaptive anti-oxidant response.

Beside their role in energy production and redox balance, mitochondria act as important spatio-temporal buffers for cytosolic Ca^{2+} due to their high membrane potential and close proximity to Ca^{2+} channels in the sarcoplasmic reticulum and sarcolemma (Ichas & Mazat, 1998; Giacomello *et al.* 2007; Rizzuto *et al.* 2009). This property is relevant in the context of DMD, as it may allow muscle cells to limit the pathological increases in cytosolic Ca^{2+}. However, the extent to which mitochondria can successfully buffer cytosolic Ca^{2+} is ultimately set by their threshold to opening of the PTP. In the present study, we report that despite being normal with respect to basal respiratory properties, mitochondria within permeabilized *mdx* fibres are more prone to opening of the PTP when exposed to Ca^{2+} overload. It should, however, be noted that a previous study performed in 5- to 6-week-old *mdx* mice reported no change in the Ca^{2+} threshold for PTP opening between control and *mdx* muscle (Reutenauer *et al.* 2008). Although the reason for this discrepancy remains unclear, one possibility is that in this prior study mitochondria were isolated using tissue homogenization and differential centrifugation, which may tend to retain healthy mitochondria and eliminate more fragile organelles (Picard *et al.* 2011). This is particularly relevant for the study of the PTP, as it is well known that the sensitivity to permeability transition is heterogeneous across the population of mitochondria within a cell, and that shifts in the proportion of sensitive *vs.* resistant mitochondria will directly influence the average PTP sensitivity of the overall population (Bernardi, 1999). In the present study, our use of a less disruptive approach to study mitochondrial function in permeabilized fibres probably allowed preservation of mitochondria that were prone to Ca^{2+}-induced PTP opening. Taken together, our results thus suggest that sensitization to permeability transition early in the course of the disease may reduce the ability of mitochondria to buffer cellular Ca^{2+} and predispose to activation of proteolytic and mitochondria-mediated cell death pathways (Bernardi *et al.* 1999; Burelle *et al.* 2010), both of which were observed in *mdx* muscles in the present study.

Effects of PGC1α gene transfer on mitochondrial function in dystrophin-deficient muscle

This is the first study to show that forced overexpression of PGC1α after the first onset of myonecrosis is able to reverse the loss of mitochondrial biomass normally observed in the TA muscle of *mdx* mice. Importantly, we also provide novel evidence indicating that PGC1α overexpression restores the resistance of mitochondria to Ca^{2+}-induced PTP opening, and thereby substantially increases the amount of Ca^{2+} that can be accumulated within mitochondria without triggering mitochondrial membrane permeabilization. Therefore, PGC1α overexpression appears to provide muscle fibres with a greater mitochondrial 'sink' to temporarily buffer excessive intracellular Ca^{2+} levels typically associated with DMD. This is consistent with the well-documented role of PGC1α as a master regulator of mitochondrial biogenesis (Kelly & Scarpulla, 2004), and with results from recent cell culture models showing the ability of PGC1α to increase the distribution volume of Ca^{2+} within mitochondria, and protect against Ca^{2+}-induced cell death (Bianchi *et al.* 2006). At the level of individual dystrophic muscle fibres, these improvements may limit injury by helping to prevent the energy deficiency previously reported in dystrophin-deficient muscle (Dunn *et al.* 1993; Even *et al.* 1994; Chen *et al.* 2000). In addition, PGC1α overexpression may prevent the activation of mitochondria-mediated cell death signalling induced by opening of the PTP, which is known to occur in other models of muscular dystrophy (Irwin *et al.* 2003; Millay *et al.* 2008; Reutenauer *et al.* 2008). This would be consistent with our observation that PGC1α gene transfer reduced the activity/levels of calpain as well as caspases 3 and 9, which respectively indicate a blunting of Ca^{2+}- and mitochondria-dependent proteolytic signalling in dystrophin-deficient muscle. Importantly, although PGC1α overexpression is known to promote fast to slow fibre type transition (Selsby *et al.* 2012), this rescue effect of PGC1α on mitochondrial function is unlikely to be explained by the well-known differences in mitochondrial content and function between fast and slow fibres (Picard *et al.* 2008*a*). Indeed, compared with fast glycolytic fibres, slow oxidative fibres display an enhanced susceptibility to PTP opening (Picard *et al.* 2008*a*) and increased activities of numerous apoptotic proteins including calpain, caspase 3 and caspase 9 (McMillan & Quadrilatero, 2011), a phenotype that is clearly opposite to the one observed in *mdx* muscle following PGC1α transfection. Finally, although PGC1α is a key modulator of mitochondrial function, we cannot exclude the possibility that some of the benefits are also partly attributable to other effects of PGC1α, such as better preservation of sarcolemmal and neuromuscular junction (NMJ) integrity through the upregulation of utrophin and NMJ-related genes (Handschin *et al.* 2007), or effects on Ca^{2+}–calmodulin signalling (Chakkalakal *et al.* 2006).

Conclusion

In summary, skeletal muscles from dystrophin-deficient animals exhibit several mitochondrial functional abnormalities early in the disease, including a lower mitochondrial biomass, a compensatory anti-oxidant response and an increased vulnerability to mitochondrial permeabilization via PTP opening when faced with a Ca^{2+} challenge. Importantly, short-term treatment with PGC1α gene transfer during the early post-necrotic phase was able to restore mitochondrial biomass to the level observed in normal healthy muscle, normalize the resistance to PTP opening and increase the capacity of mitochondria to buffer Ca^{2+}. This was associated with a mitigation of Ca^{2+}-dependent proteolytic (calpain) and apoptotic (caspases 3/9) signalling in dystrophic muscles. Taken together, these data suggest that treatments aimed at increasing PGC1α signalling may protect dystrophin-deficient muscles by stimulating mitochondrial biogenesis and providing a Ca^{2+} sink to limit Ca^{2+}-related cellular abnormalities, as well as by preventing the activation of cell death pathways associated with mitochondrial permeabilization.

References

Anderson E & Neufer P (2006). Type II skeletal myofibers possess unique properties that potentiate mitochondrial H_2O_2 generation. *Am J Physiol Cell Physiol* **290**, C844–C851.

Ascah A, Khairallah M, Daussin F, Bourcier-Lucas C, Godin R, Allen BG, Petrof BJ, Rosiers Des C & Burelle Y (2011). Stress-induced opening of the permeability transition pore in the dystrophin-deficient heart is attenuated by acute treatment with sildenafil. *Am J Physiol Heart Circ Physiol* **300**, H144–H153.

Bernardi P (1999). Mitochondrial transport of cations: channels, exchangers, and permeability transition. *Physiol Rev* **79**, 1127–1155.

Bernardi P, Scorrano L, Colonna R, Petronilli V & Di Lisa F (1999). Mitochondria and cell death. Mechanistic aspects and methodological issues. *Eur J Biochem* **264**, 687–701.

Bianchi K, Vandecasteele G, Carli C, Romagnoli A, Szabadkai G & Rizzuto R (2006). Regulation of Ca^{2+} signalling and Ca^{2+}-mediated cell death by the transcriptional coactivator PGC-1α. *Cell Death Differ* **13**, 586–596.

Briguet A, Courdier-Fruh I, Foster M, Meier T & Magyar JP (2004). Histological parameters for the quantitative assessment of muscular dystrophy in the mdx-mouse. *Neuromuscul Disord* **14**, 675–682.

Brookes P, Yoon Y, Robotham J, Anders M & Sheu S (2004). Calcium, ATP, and ROS: a mitochondrial love-hate triangle. *Am J Physiol Cell Physiol* **287**, C817–C833.

Burelle Y, Khairallah M, Ascah A, Allen BG, Deschepper CF, Petrof BJ & Rosiers Des C (2010). Alterations in mitochondrial function as a harbinger of cardiomyopathy: lessons from the dystrophic heart. *J Mol Cell Cardiol* **48**, 310–321.

Carreira RS, Lee Y, Ghochani M, Gustafsson AB & Gottlieb RA (2010). Cyclophilin D is required for mitochondrial removal by autophagy in cardiac cells. *Autophagy* **6**, 462–472.

Chakkalakal JV, Michel SA, Chin ER, Michel RN & Jasmin BJ (2006). Targeted inhibition of Ca^{2+}/calmodulin signaling exacerbates the dystrophic phenotype in mdx mouse muscle. *Hum Mol Genet* **15**, 1423–1435.

Chen Y, Zhao P, Borup R & Hoffman E (2000). Expression profiling in the muscular dystrophies: identification of novel aspects of molecular pathophysiology. *J Cell Biol* **151**, 1321–1336.

Csukly K, Ascah A, Matas J, Gardiner PF, Fontaine E & Burelle Y (2006). Muscle denervation promotes opening of the permeability transition pore and increases the expression of cyclophilin D. *J Physiol* **574**, 319–327.

Dudley RWR, Danialou G, Govindaraju K, Lands L, Eidelman DE & Petrof BJ (2006*a*). Sarcolemmal damage in dystrophin deficiency is modulated by synergistic interactions between mechanical and oxidative/nitrosative stresses. *Am J Pathol* **168**, 1276–1287.

Dudley RWR, Khairallah M, Mohammed S, Lands L, Rosiers Des C & Petrof BJ (2006*b*). Dynamic responses of the glutathione system to acute oxidative stress in dystrophic mouse (mdx) muscles. *Am J Physiol Regul Integr Comp Physiol* **291**, R704–R710.

Dunn JF, Tracey I & Radda GK (1993). Exercise metabolism in Duchenne muscular dystrophy: a biochemical and [^{31}P]-nuclear magnetic resonance study of mdx mice. *Proc Biol Sci* **251**, 201–206.

Elmore SP, Qian T, Grissom SF & Lemasters JJ (2001). The mitochondrial permeability transition initiates autophagy in rat hepatocytes. *FASEB J* **15**, 2286–2287.

Even PC, Decrouy A & Chinet A (1994). Defective regulation of energy metabolism in mdx-mouse skeletal muscles. *Biochem J* **304**, 649–654.

Fraysse B, Nagi SM, Boher B, Ragot H, Lainé J, Salmon A, Fiszman MY, Toussaint M & Fromes Y (2010). Ca^{2+} overload and mitochondrial permeability transition pore activation in living delta-sarcoglycan-deficient cardiomyocytes. *Am J Physiol Cell Physiol* **299**, C706–C713.

Gannoun-Zaki L, Fournier-Bidoz S, Le Cam G, Chambon C, Millasseau P, Léger JJ & Dechesne CA (1995). Down-regulation of mitochondrial mRNAs in the mdx mouse model for Duchenne muscular dystrophy. *FEBS Lett* **375**, 268–272.

Giacomello M, Drago I, Pizzo P & Pozzan T (2007). Mitochondrial Ca^{2+} as a key regulator of cell life and death. *Cell Death Differ* **14**, 1267–1274.

Gillis JM (1999). Understanding dystrophinopathies: an inventory of the structural and functional consequences of the absence of dystrophin in muscles of the mdx mouse. *J Muscle Res Cell Motil* **20**, 605–625.

Glesby MJ, Rosenmann E, Nylen EG & Wrogemann K (1988). Serum CK, calcium, magnesium, and oxidative phosphorylation in mdx mouse muscular dystrophy. *Muscle Nerve* **11**, 852–856.

Gottlieb RA & Carreira RS (2010). Autophagy in health and disease. 5. Mitophagy as a way of life. *Am J Physiol Cell Physiol* **299**, C203–C210.

Gottlieb RA & Mentzer RM (2011). Cardioprotection through autophagy: ready for clinical trial? *Autophagy* **7**, 434–435.

Handschin C, Kobayashi YM, Chin S, Seale P, Campbell KP & Spiegelman BM (2007). PGC-1a regulates the neuromuscular junction program and ameliorates Duchenne muscular dystrophy. *Genes Dev* **21**, 770–783.

Ichas F, Jouaville L & Mazat J (1997). Mitochondria are excitable organelles capable of generating and conveying electrical and calcium signals. *Cell* **89**, 1145–1153.

Ichas F & Mazat J (1998). From calcium signaling to cell death: two conformations for the mitochondrial permeability transition pore. Switching from low- to high-conductance state. *Biochim Biophys Acta* **1366**, 33–50.

Irwin WA, Bergamin N, Sabatelli P, Reggiani C, Megighian A, Merlini L, Braghetta P, Columbaro M, Volpin D, Bressan GM, Bernardi P & Bonaldo P (2003). Mitochondrial dysfunction and apoptosis in myopathic mice with collagen VI deficiency. *Nat Genet* **35**, 367–371.

Javadov S, Clarke S, Das M, Griffiths E, Lim K & Halestrap A (2003). Ischaemic preconditioning inhibits opening of mitochondrial permeability transition pores in the reperfused rat heart. *J Physiol* **549**, 513–524.

Kelly DP & Scarpulla RC (2004). Transcriptional regulatory circuits controlling mitochondrial biogenesis and function. *Genes Dev* **18**, 357–368.

Koenig M, Hoffman EP, Bertelson CJ, Monaco AP, Feener C & Kunkel LM (1987). Complete cloning of the Duchenne muscular dystrophy (DMD) cDNA and preliminary genomic organization of the DMD gene in normal and affected individuals. *Cell* **50**, 509–517.

Kornegay JN, Childers MK, Bogan DJ, Bogan JR, Nghiem P, Wang J, Fan Z, Howard JF, Schatzberg SJ, Dow JL, Grange RW, Styner MA, HOFFMAN EP & Wagner KR (2012). The paradox of muscle hypertrophy in muscular dystrophy. *Phys Med Rehabil Clin N Am* **23**, 149–172.

Kuznetsov AV, Winkler K, Wiedemann FR, Bossanyi von P, Dietzmann K & Kunz WS (1998). Impaired mitochondrial oxidative phosphorylation in skeletal muscle of the dystrophin-deficient mdx mouse. *Mol Cell Biochem* **183**, 87–96.

McMillan EM & Quadrilatero J (2011). Differential apoptosis-related protein expression, mitochondrial properties, proteolytic enzyme activity, and DNA fragmentation between skeletal muscles. *Am J Physiol Regul Integr Comp Physiol* **300**, R531–R543.

Marcil M, Ascah A, Matas J, Bélanger S, Deschepper CF & Burelle Y (2006). Compensated volume overload increases the vulnerability of heart mitochondria without affecting their functions in the absence of stress. *J Mol Cell Cardiol* **41**, 998–1009.

Millay DP, Sargent MA, Osinska H, Baines CP, Barton ER, Vuagniaux G, Sweeney HL, Robbins J & Molkentin JD (2008). Genetic and pharmacologic inhibition of mitochondrial-dependent necrosis attenuates muscular dystrophy. *Nat Med* **14**, 442–447.

Molnar MJ, Gilbert R, Lu Y, Liu AB, Guo A, Larochelle N, Orlopp K, Lochmuller H, Petrof BJ, Nalbantoglu J & Karpati G (2004). Factors influencing the efficacy, longevity, and safety of electroporation-assisted plasmid-based gene transfer into mouse muscles. *Mol Ther.* Sep; **10**(3), 447–455.

Mouisel E, Vignaud A, Hourdé C, Butler-Browne G & Ferry A (2010). Muscle weakness and atrophy are associated with decreased regenerative capacity and changes in mTOR signaling in skeletal muscles of venerable (18–24-month-old) dystrophic mdx mice. *Muscle Nerve* **41**, 809–818.

Petrof B (2002). Molecular pathophysiology of myofiber injury in deficiencies of the dystrophin-glycoprotein complex. *Am J Phys Med Rehabil* **81**, S162–S174.

Petrof BJ, Shrager JB, Stedman HH, Kelly AM & Sweeney HL (1993*a*). Dystrophin protects the sarcolemma from stresses developed during muscle contraction. *Proc Natl Acad Sci U S A* **90**, 3710–3714.

Petrof BJ, Stedman HH, Shrager JB, Eby J, Sweeney HL & Kelly AM (1993*b*). Adaptations in myosin heavy chain expression and contractile function in dystrophic mouse diaphragm. *Am J Physiol Cell Physiol* **265**, C834–C841.

Picard M, Csukly K, Robillard M-E, Godin R, Ascah A, Bourcier-Lucas C & Burelle Y (2008*a*). Resistance to Ca^{2+}-induced opening of the permeability transition pore differs in mitochondria from glycolytic and oxidative muscles. *Am J Physiol Regul Integr Comp Physiol* **295**, R659–R668.

Picard M, Godin R, Sinnreich M, Baril J, Bourbeau J, Perrault H, Taivassalo T & Burelle Y (2008*b*). The mitochondrial phenotype of peripheral muscle in chronic obstructive pulmonary disease: disuse or dysfunction? *Am J Respir Crit Care Med* **178**, 1040–1047.

Picard M, Taivassalo T, Gouspillou G & Hepple RT (2011). Mitochondria: isolation, structure and function. *J Physiol* **589**, 4413–4421.

Reutenauer J, Dorchies OM, Patthey-Vuadens O, Vuagniaux G & Ruegg UT (2008). Investigation of Debio 025, a cyclophilin inhibitor, in the dystrophic mdx mouse, a model for Duchenne muscular dystrophy. *Br J Pharmacol* **155**, 574–584.

Rizzuto R, Marchi S, Bonora M, Aguiari P, Bononi A, De Stefani D, Giorgi C, Leo S, Rimessi A, Siviero R, Zecchini E & Pinton P (2009). Ca^{2+} transfer from the ER to mitochondria: when, how and why. *Biochim Biophys Acta* **1787**, 1342–1351.

Ruegg UT, Nicolas-Métral V, Challet C, Bernard-Hélary K, Dorchies OM, Wagner S & Buetler TM (2002). Pharmacological control of cellular calcium handling in dystrophic skeletal muscle. *Neuromuscul Disord* **12**, S155–S161.

Selsby JT, Morine KJ, Pendrak K, Barton ER & Sweeney HL (2012). Rescue of dystrophic skeletal muscle by PGC-1α involves a fast to slow fiber type shift in the mdx mouse. *PLoS ONE* **7**, e30063.

Tidball JG & Wehling-Henricks M (2007). The role of free radicals in the pathophysiology of muscular dystrophy. *J Appl Physiol* **102**, 1677–1686.

Turrens JF (2003). Mitochondrial formation of reactive oxygen species. *J Physiol (Lond)* **552**, 335–344.

Wang W, Fang H, Groom L, Cheng A, Zhang W, Liu J *et al.* (2008). Superoxide flashes in single mitochondria. *Cell* **134**, 279–290.

Webster C, Silberstein L, Hays AP & Blau HM (1988). Fast muscle fibers are preferentially affected in Duchenne muscular dystrophy. *Cell* **52**, 503–513.

Zamzami N, Larochette N & Kroemer G (2005). Mitochondrial permeability transition in apoptosis and necrosis. *Cell Death Differ* **12** Suppl 2, 1478–1480.

Author contributions

F.D. and R.G. performed the experiments performed data analysis and drafted the manuscript. S.M. participated in the study design. T.L. performed some experiments. B.J.P. designed the study, provided the expertise for electroporation of PGC1α and critically reviewed the manuscript. Y.B. designed and supervised the study and wrote the manuscript. All authors approved the final version for publication.

Acknowledgements

This work was funded by a grant from the Canadian Institutes of Health Research to B.J.P and Y.B. Y.B. is a Junior II Investigator of the Fonds de Recherche en Santé du Québec (FRSQ). The authors would like to thank Johanne Bourdon, Christian Lemaire and Gilles Gouspillou for expert technical help.

Translational perspective

Duchenne muscular dystrophy (DMD), the most frequent form of dystrophy in humans, is caused by mutations of the dystrophin gene. Although achieving therapeutic restoration of dystrophin is an area of active research, modulation of secondarily affected cellular functions that play a major role in disease pathogenesis, represents another promising therapeutic approach. In this regard, overexpression of the transcriptional coactivator PGC1α, a master regulator of mitochondrial biogenesis, was recently shown to mitigate pathology in dystrophic muscles, through mechanisms that are not fully understood. Using the *mdx* mouse model of DMD, we tested the hypothesis that mitochondrial dysfunction represents an early event in the pathogenesis of DMD, and that overexpression of PGC1α

shortly after the onset of myofibre necrosis, is able to rescue mitochondrial functional abnormalities. Our results reveal that dystrophin-deficient muscle displays multiple mitochondrial abnormalities at baseline including reduced mitochondrial content and an increased susceptibility to Ca^{2+}-induced opening of the permeability transition pore (a key event in necrotic cell death signalling). Plasmid-mediated transfection of PGC1α in *mdx* muscles not only increases mitochondrial content but also reduces permeability transition pore opening, improves mitochondrial Ca^{2+} handling, and decreases the activation of Ca^{2+} and mitochondria-dependent proteases. Overall, this study provides further evidence for the contribution of mitochondrial functional abnormalities to the pathogenesis of DMD, as well as mechanistic insights into the therapeutic potential of strategies aimed at increasing PGC1α expression and mitochondrial biogenesis in dystrophin-deficient muscles.